This article was downloaded by:
On: *21 January 2011*
Access details: *Access Details: Free Access*
Publisher *Taylor & Francis*
Informa Ltd Registered in England and Wales Registered Number: 1072954 Registered office: Mortimer House, 37-41 Mortimer Street, London W1T 3JH, UK

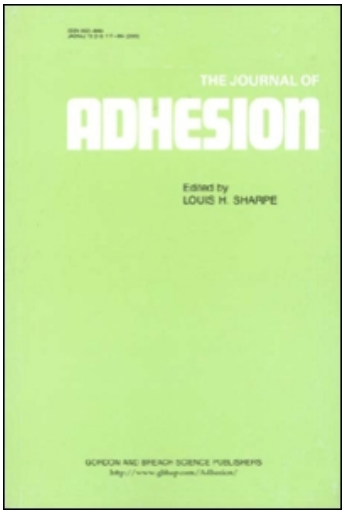

The Journal of Adhesion
Publication details, including instructions for authors and subscription information:
http://www.informaworld.com/smpp/title~content=t713453635

Stress Analysis of Shaft-Tube Bonded Joints Using a Variational Method

S. Kumar[a]; J. P. Scanlan[b]
[a] Solid Mechanics and Materials Engineering Group, Department of Engineering Science, University of Oxford, Oxford, UK [b] Computational Engineering and Design Centre, School of Engineering Sciences, University of Southampton, Southampton, UK

Online publication date: 15 April 2010

To cite this Article Kumar, S. and Scanlan, J. P.(2010) 'Stress Analysis of Shaft-Tube Bonded Joints Using a Variational Method', The Journal of Adhesion, 86: 4, 369 — 394
To link to this Article: DOI: 10.1080/00218461003704329
URL: http://dx.doi.org/10.1080/00218461003704329

PLEASE SCROLL DOWN FOR ARTICLE

Full terms and conditions of use: http://www.informaworld.com/terms-and-conditions-of-access.pdf

This article may be used for research, teaching and private study purposes. Any substantial or systematic reproduction, re-distribution, re-selling, loan or sub-licensing, systematic supply or distribution in any form to anyone is expressly forbidden.

The publisher does not give any warranty express or implied or make any representation that the contents will be complete or accurate or up to date. The accuracy of any instructions, formulae and drug doses should be independently verified with primary sources. The publisher shall not be liable for any loss, actions, claims, proceedings, demand or costs or damages whatsoever or howsoever caused arising directly or indirectly in connection with or arising out of the use of this material.

The Journal of Adhesion, 86:369–394, 2010
Copyright © Taylor & Francis Group, LLC
ISSN: 0021-8464 print/1545-5823 online
DOI: 10.1080/00218461003704329

Taylor & Francis
Taylor & Francis Group

Stress Analysis of Shaft-Tube Bonded Joints Using a Variational Method

S. Kumar[1] and J. P. Scanlan[2]
[1]Solid Mechanics and Materials Engineering Group, Department of Engineering Science, University of Oxford, Oxford, UK
[2]Computational Engineering and Design Centre, School of Engineering Sciences, University of Southampton, Southampton, UK

Downloaded At: 19:34 21 January 2011

Functionally modulus graded bondline (FMGB) adhesives can be employed in bonded joints to reduce stress concentration and, hence, achieve higher joint strength. This study presents an analytical framework for the stress analysis of a shaft-tube bonded joint based on a variational technique which minimises the complimentary energy of the bonded system. This cylindrical assembly consists of similar or dissimilar adherends and a FMGB adhesive. The effect of functional grading of adhesive elastic modulus on the peak stresses and their distributions in the adhesive layer are studied. The joint with various modulus grading profiles is assessed and the results are compared with a conventional mono-modulus bondline (MMB) adhesive joint. Stress analysis indicates that the peel and shear peak stresses in the FMGB are much smaller and their distributions along bondlength are more uniform than those of MMB adhesive joints under the same axial tensile load. Numerical examples are provided to illustrate the effects of geometrical and material properties on the distributions and intensities of stresses in the bondline. Furthermore, optimal peel and shear strengths of the joint can be achieved by spatially controlling the modulus of the adhesive.

Keywords: Adhesive joint; Functionally modulus graded bondline; Stress analysis; Stress concentration; Variational method

1. NOMENCLATURE

E_{l1}, E_{t1}, ν_{tl1}, G_1	Transversely isotropic shaft properties
E_{2l}, E_{2t}, ν_{tl2}, G_2	Transversely isotropic tube properties

Received 14 June 2009; in final form 20 October 2009.

Address correspondence to S. Kumar, Solid Mechanics and Materials Engineering Group, Department of Engineering Science, Oxford University, Parks Road, Oxford, OX1 3JP, United Kingdom. E-mail: kumar.shanmugam@eng.ox.ac.uk

E_1, ν_1	Young's modulus and Poisson's ratio of the shaft, respectively
E_2, ν_2	Young's modulus and Poisson's ratio of the tube, respectively
E, ν	Young's modulus and Poisson's ratio of the MMB adhesive, respectively
E_{f1}, E_{f2}, E_{f3}, E_{f4}	Modulus functions of the FMGB adhesive
E_m, E_o	Maximum and minimum values of Young's modulus of the FMGB adhesive
$E(z)$	Arbitrary modulus function of the FMGB adhesive
b	Radius of the shaft
c, d	Inner and outer radii of the tube respectively
t_2	Thickness of the tube
t	Thickness of the adhesive layer
P	Axial tensile load
L	Bond length of the joint
η	Normalised bond length of the joint
r, θ, z	Radial, circumferential, and axial coordinates of the tubular system, respectively
q, f	Axial edge stresses in the shaft and tube of the jointed portion, respectively
$\sigma_{rr}^{(1)}, \sigma_{\theta\theta}^{(1)}, \sigma_{zz}^{(1)}, \tau_{rz}^{(1)}$	Stress components in the shaft
$\sigma_{rr}^{(2)}, \sigma_{\theta\theta}^{(2)}, \sigma_{zz}^{(2)}, \tau_{rz}^{(2)}$	Stress components in the tube
σ_{rr}, $\sigma_{\theta\theta}$, σ_{zz}, τ_{rz}	Stress components in the adhesive
Π_1, Π_2, Π_3	Complementary energy in the shaft, tube, and adhesive, respectively
Π	Complementary energy of the bonded system

Downloaded At: 19:34 21 January 2011

2. INTRODUCTION

Adhesively bonded joints are widely used in a variety of industries for joining dissimilar materials since they provide more uniform load transfer over the bonded area. Weight reduction and improved fatigue life are the drivers for the extensive use of adhesively bonded joints. Numerous studies have been devoted to the stress analysis of bonded joints, both analytically and numerically, forming the basis for design and durability assessment of joints [1–14].

There are several types of tubular lap joints such as single lap joint, double lap joint, stepped lap joint, scarf lap joint, etc. Out of these, the tubular single lap joint is the most occuring one due to its ease of manufacture and its low cost. Initially, Lubkin and Reissner [1]

analysed the stress distribution in the adhesive of tubular lap joints composed of thin-walled circular cylindrical shell elements subjected to axisymmetric loading, with the assumptions that the adhesive is thin and much more flexible than the adherends. They treated the adhesive as a series of infinitesimal coil springs. Later, the same problem was verified using axisymmetric quadratic isoparametric finite elements by Adams and Peppiatt [8]. Adams and Peppiatt also analysed tubular lap joints under torsional loads.

A few researchers have proposed two-dimensional analytical solutions for cylindrical bonded joints, which were focused on the joint overlap, ensuring the stress-free boundary conditions at the free ends. For instance, Allman [15] used a minimum strain energy, with given bending, stretching and shearing at the end of the overlap and assuming that the longitudinal normal stress was zero, the shear stress constant, and the transverse normal stress was linearly distributed across the thickness of the adhesive. Shi and Cheng [16] presented approximate closed form solutions for tubular bonded joints based on the variational principle of complementary energy with similar boundary conditions and assumptions to those of Allman. Lindon *et al.* [17] presented experimental and theoretical investigations to calculate the strength of cylindrical assemblies with an anaerobic adhesive. Pugno and Carpinteri [18] analysed static and dynamic behaviour of tubular adhesive joints under axial load. Imanaka *et al.* [19] proposed a method of fatigue strength estimation of adhesive bonded shaft joints based on experimental and finite element studies. Nayeb-Hashemi *et al.* [20] proposed a damage model for tubular joints under combined axial and torsional cyclic loading. Thomsen [21] carried out elasto-plastic numerical stress analysis of tubular lap joints comprising dissimilar orthotropic circular cylindrical laminated shells under non-axisymmetric type of loading and showed that the inelastic behaviour of the adhesive affects the adhesive stress distribution even at low levels of external loading. Kim *et al.* [22] included nonlinear properties and fabrication residual thermal stresses in the stress calculation of tubular single-lap carbon/epoxy composite-steel joints. Recently, Nemes *et al.* [23] provided a statically determinate elastic solution for the cylindrical lap joint employing the same methodology as that of Shi and Cheng [16]. In this study, a theoretical framework has been provided for the stress analysis of a shaft-tube joint with a FMGB adhesive.

Several techniques have been used to minimise the stress concentrations at the ends of the overlap of single lap joints and, hence, to improve structural capability [24–26]. These include altering the

Downloaded At: 19:34 21 January 2011

adherend geometry [27–29], the adhesive geometry [30], and the spew geometry [31,32]. These studies mostly focused on the geometrical aspects of adhesive and adherends to minimise stress concentration. Nevertheless, in a few cases, change of geometry is limited by complexities involved in production, besides the cost. A few researchers altered the material of the adhesive globally to achieve higher joint strength. They studied the effect of the shear modulus of the adhesive on the shear stress distribution in the bondline and showed that it has a considerable effect [24,33]. Sadek [34] has shown that the lap-shear strength of the joints can be enhanced by introducing a stiff adhesive in the bondline. However, in this case, adhesives are prone to interfacial brittle failure owing to the high peel stresses they experience. Even if a compliant adhesive is employed in the bondline, the stress distribution in the bonded area would be non-uniform [34]. On the other hand, swapping the material of the adherends would not be possible because the adherend material is selected based on the functional requirement of the structural members to be bonded. However, the material properties of the adherends or adhesive can be altered in the overlap region. Ganesh *et al.* [35] showed that composite materials with continuously varying material properties can be fabricated by modifying the conventional braiding technology of fiber placement. Boss *et al.* [36] studied the stress distribution in the adhesive of a single lap joint with a modulus and geometrically graded composite adherend. Recently, Pires *et al.* [37,38] and Fitton and Broughton [39] have evaluated performance of bi-adhesive bonded lap joints and have shown considerable increase in joint strength compared with mono-adhesive joints. Temiz [40] numerically examined bi-adhesive double-strap joints under a bending moment. Kumar and Pandey [41] performed 2-D and 3-D FE studies on bi-adhesive single lap joints and showed that the 3-D analysis is indispensable for the design of such joints. Recently, Kumar [42] has provided analytical framework to study the stress distribution in functionally modulus graded bondline (FMGB) adhesive joints. Da Silva and Adams [43] have shown that at high and low temperatures joint strengths can be significantly improved if dissimilar adherends along with dual adhesives are employed. All these investigators have considered only a one-step variation in adhesive modulus over the bondlength. Therefore, in this study, a multi-step variation of the modulus of the adhesive along its length has been considered, so as to reduce peel and shear stress peaks and to minimise their non-uniform distribution in the bondline. The task is to formulate the adhesive and adherends stresses in terms of geometrical and mechanical properties of the shaft-tube assembly.

Downloaded At: 19:34 21 January 2011

3. PROBLEM FORMULATION

Consider a shaft and a tube of different materials as shown in Fig. 1 (Left). The two members are lap-jointed by a FMGB adhesive. This cylindrical assembly is subjected to an axial tensile load, P. Figure 1 (Right) shows the coordinate system with coordinates r and z and the edge stresses (q and f) of the bonded portion whose length is L. The objective of the problem is to find the stress distribution in the adhesive layer when using an adhesive whose elastic modulus varies along the length of the bond.

The following assumptions have been adopted to analyse this axisymmetric bonded system.

- The radial stresses in all the three domains of the cylindrical assembly are neglected ($\sigma_{rr}^{(1)} = \sigma_{rr}^{(2)} = \sigma_{rr} = 0$).
- Axisymmetric condition implies that the following shear stresses are zero ($\tau_{r\theta}^{(1)} = \tau_{z\theta}^{(1)} = 0, \tau_{r\theta}^{(2)} = \tau_{z\theta}^{(2)} = 0, \tau_{r\theta} = \tau_{z\theta} = 0$) in all three domains.
- For a thin adhesive, the difference between the two shearing stresses [the one acting on the outer surface of the adhesive $\tau_{rz}(c, z)$ and the other acting on the inner surface of the adhesive $\tau_{rz}(b, z)$] is very small and, hence, the longitudinal stress, σ_{zz}, in the adhesive may be neglected as compared with the shearing stress, τ_{rz}.
- The longitudinal stress in the shaft and the tube is a function of the axial coordinate z only, *i.e.*, $\sigma_{zz}^{(1)} = \sigma_{zz}^{(1)}(z); \sigma_{zz}^{(2)} = \sigma_{zz}^{(2)}(z)$.

Therefore, the non-zero stress components in the cylindrical assembly are:

- Shaft: $\tau_{rz}^{(1)}(r,z), \sigma_{\theta\theta}^{(1)}(r,z), \sigma_{zz}^{(1)}(z)$

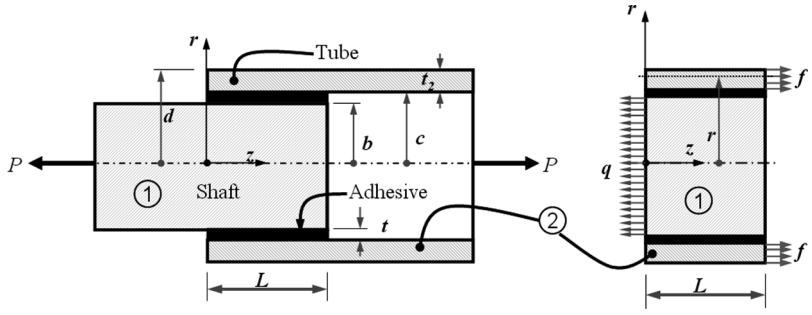

FIGURE 1 Left: Adhesively bonded shaft-tube joint; Right: Coordinate system (r, θ, z) and edge stresses on jointed portion.

Downloaded At: 19:34 21 January 2011

- Adhesive: $\tau_{rz}(r, z)$, $\sigma_{\theta\theta}(r, z)$
- Tube: $\tau_{rz}^{(2)}(r,z), \sigma_{\theta\theta}^{(2)}(r,z), \sigma_{zz}^{(2)}(z)$.

Incorporating the aforementioned assumptions, the differential equations of equilibrium are reduced to the following and are valid in all the three domains:

$$\frac{\partial \tau_{rz}}{\partial z} - \frac{1}{r}\sigma_{\theta\theta} = 0 \tag{1}$$

$$\frac{\partial \tau_{rz}}{\partial z} + \frac{\partial \sigma_{zz}}{\partial z} + \frac{1}{r}\tau_{rz} = 0. \tag{2}$$

In this investigation, stress analysis of the shaft-tube joint is presented based on admissible stress field that satisfy the equilibrium equations and the stress boundary conditions at $z = 0$, $z = L$, and the stress continuity at the interfaces ($r = b$; $r = c$). The equilibrium of the assembly dictates the following relationship between q and f and $\sigma_{zz}^{(1)}$ and $\sigma_{zz}^{(2)}$:

$$P = q\pi b^2 = f\pi(d^2 - c^2) = \sigma_{zz}^{(1)}\pi b^2 + \sigma_{zz}^{(2)}\pi(d^2 - c^2) \tag{3}$$

$$\sigma_{zz}^{(2)} = f + \frac{b^2}{(c^2 - d^2)}\sigma_{zz}^{(1)}. \tag{4}$$

3.1. Stress Fields in the Adherends and the Adhesive

Considering equilibrium of an elemental length, dz, of the shaft as shown in Fig. 2a, the shear stress, $\tau_{rz}^{(1)}$, in the shaft can be expressed as

$$\tau_{rz}^{(1)}(r,z) = \frac{r}{2}\frac{d\sigma_{zz}^{(1)}}{dz}. \tag{5}$$

Using $\tau_{rz}^{(1)}$ given by Eq. (5) in equilibrium Eq. (1), we can get the tangential stress in the shaft which is given by

$$\sigma_{\theta\theta}^{(1)}(r,z) = \frac{r^2}{2}\frac{d^2\sigma_{zz}^{(1)}}{dz^2}. \tag{6}$$

Similarly, considering equilibrium of the elemental length, dz, of the shaft and the adhesive together as depicted in Fig. 2b, we can express τ_{rz} as

$$\tau_{rz}(r,z) = \frac{b^2}{2r}\frac{d\sigma_{zz}^{(1)}}{dz}. \tag{7}$$

Downloaded At: 19:34 21 January 2011

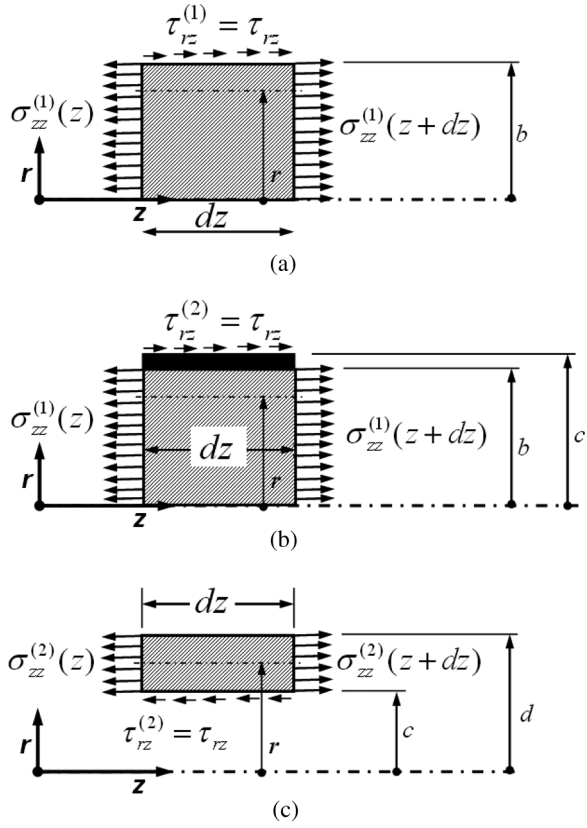

FIGURE 2 (a) Equilibrium of the shaft; (b) equilibrium of the shaft and adhesive; (c) equilibrium of the tube.

Again, using τ_{rz} in equilibrium Eq. (1), the circumferential stress, $\sigma_{\theta\theta}$, in the adhesive is obtained as

$$\sigma_{\theta\theta}(r,z) = \frac{b^2}{2}\frac{d^2\sigma_{zz}^{(1)}}{dz^2}. \tag{8}$$

Note that the circumferential stress in the adhesive is independent of r since we assumed that σ_{zz} is negligible. Considering equilibrium of elemental length, dz, of the tube as shown in Fig. 2c, the shear stress in the tube can be given as a function of the gradient of longitudinal stress in the tube:

$$\tau_{rz}^{(2)}(r,z) = \frac{(r^2 - d^2)}{2r}\frac{d\sigma_{zz}^{(2)}}{dz}. \tag{9}$$

Downloaded At: 19:34 21 January 2011

Applying the shear stress continuity condition at the interfaces ($\tau_{rz}^{(2)}$ at $r=c$ is equal to τ_{rz} at $r=c$), we can relate the longitudinal stress gradients in shaft and tube as

$$\frac{d\sigma_{zz}^{(2)}}{dz} = \frac{b^2}{(c^2-d^2)}\frac{d\sigma_{zz}^{(1)}}{dz}. \tag{10}$$

Using the above in Eq. (9), we get

$$\tau_{rz}^{(2)}(r,z) = \frac{(r^2-d^2)}{2r}\frac{b^2}{(c^2-d^2)}\frac{d\sigma_{zz}^{(1)}}{dz}. \tag{11}$$

Now, either the continuity of circumferential stress condition or equilibrium equations can be used to obtain the tangential stress in the tube as

$$\sigma_{\theta\theta}^{(2)}(r,z) = \frac{(r^2-d^2)}{2}\frac{b^2}{(c^2-d^2)}\frac{d^2\sigma_{zz}^{(1)}}{dz^2}. \tag{12}$$

Downloaded At: 19:34 21 January 2011

It is clear from the above given expressions that both shear and circumferential stresses are continuous across the interfaces. Thus, the stress components in the shaft $[\tau_{rz}^{(1)}(r,z), \sigma_{\theta\theta}^{(1)}(r,z)]$, in the adhesive $[\tau_{rz}(r,\ z),\ \sigma_{\theta\theta}(r,\ z)]$, and in the tube $[\tau_{rz}^{(2)}(r,z), \sigma_{\theta\theta}^{(2)}(r,z), \sigma_{zz}^{(2)}(z)]$ are expressed in terms of a single unknown stress function, $\sigma_{zz}^{(1)}(z)$. Now, the statically determinate problem is solved applying the stress boundary conditions prescribed at the ends of overlap and the stress-free end conditions. The boundary conditions are:

$$\sigma_{zz}^{(1)}(0) = q; \quad \sigma_{zz}^{(1)}(L) = 0; \tag{13}$$

$$\tau_{rz}(r,0) = 0; \quad \tau_{rz}(r,L) = 0; \quad r \in [b,c]. \tag{14}$$

3.2. Functionally Modulus Graded Bondline (FMGB) Adhesive

A few researchers have examined the concept of a bi-adhesive bonding technique in which the stiff adhesive is applied in the middle portion of the bondline while the compliant adhesive is applied at the overlap ends. These studies indicate that bi-adhesive joints have reduced stress concentration at the overlap ends compared with traditional MMB adhesive joints. In bi-adhesive joints there is only one step variation of the elastic modulus of the adhesive along the bond length. In the current study, a multi-step variation of the modulus of the bondline adhesive is considered. A multi-modulus bondline in tubular joints can be achieved by adopting a procedure similar to that described

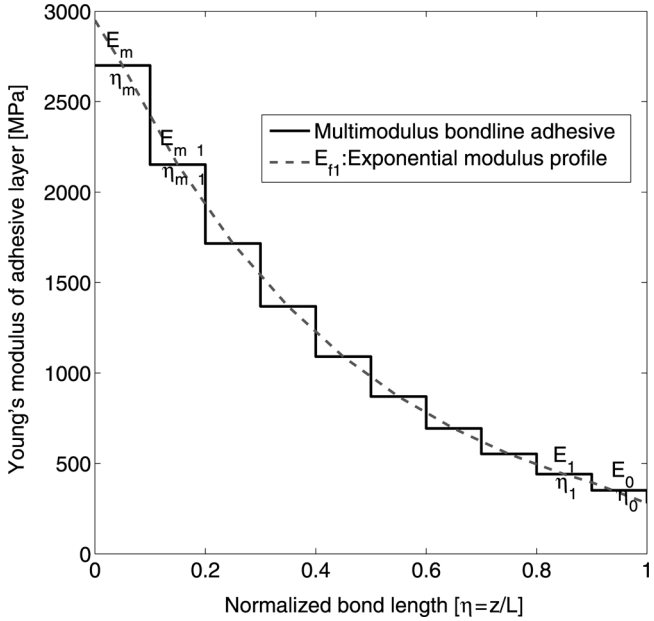

FIGURE 3 Representation of multi-modulus bondline adhesive as a functionally modulus graded bondline adhesive.

Downloaded At: 19:34 21 January 2011

by Mengel *et al.* [44]. This multi-step variation is approximated by a smoothly varying modulus function as shown in Fig. 3. The adhesive modulus is gradually reduced from the shaft end to the tube end. The modulus function is approximated such that

$$\int_0^1 E_f(\eta)\, d\eta \simeq E_0\eta_0 + E_1\eta_1 + \cdots + E_{m-1}\eta_{m-1} + E_m\eta_m. \tag{15}$$

The various modulus profiles examined in the analysis are given below and are shown in Fig. 4. These modulus functions are arbitrarily chosen.

$$E_{f1} = E_m \exp\left[\ln\left(\frac{E_o}{E_m}\right)\left(\frac{z}{L}\right)\right] \tag{16}$$

$$E_{f2} = (E_o - E_m)\left[\frac{z}{L}\right]^3 + E_m \tag{17}$$

$$E_{f3} = (E_o - E_m)\left[\frac{z}{L}\right]^2 + E_m \tag{18}$$

$$E_{f4} = E_m \tag{19}$$

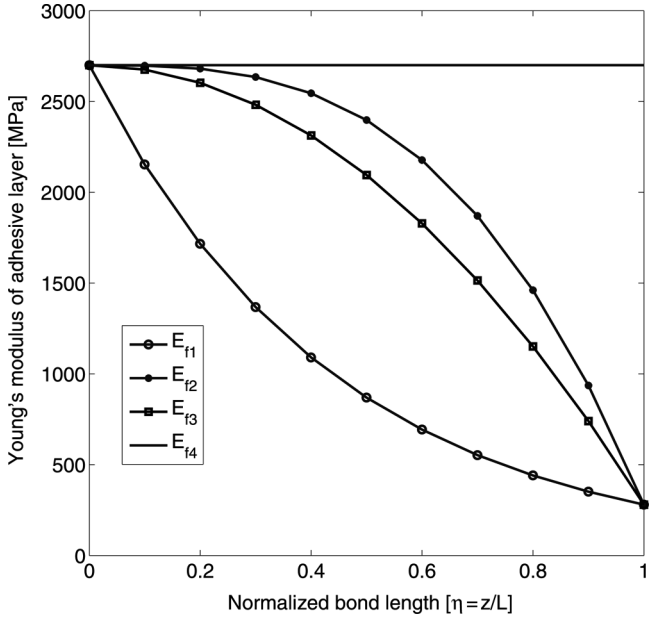

FIGURE 4 Young's modulus of adhesive as a function of normalised bondlength, η.

Downloaded At: 19:34 21 January 2011

4. VARIATIONAL METHOD

The variational analysis can be based either on an assumed infinitesimal displacement field in conjunction with the principle of minimum potential energy or on an assumed small stress variation associated with the complementary energy [45]. In this study, the second route has been pursued, following the analysis developed by Shi and Cheng [16] for tubular-lap joints and extending it to shaft-tube joint with a FMGB adhesive. The problem can be defined as obtaining a solution for the stress function $\sigma_{zz}^{(1)}$ by minimizing the complementary energy of the cylindrical bonded system, where the stress components in the adherends and in the FMGB adhesive have been expressed in terms of a single stress function, $\sigma_{zz}^{(1)}$. The admissible stress states are those that satisfy the differential equations of equilibrium, traction boundary conditions, stress-free end conditions of the joint, and stress continuity at the interfaces. Once $\sigma_{zz}^{(1)}$ has been obtained, then all the stress components in the adhesive and adherends can be obtained.

The complementary energy of the joint comprising transversely isotropic shaft and tube and a functionally modulus graded isotropic adhesive can be given by Π, where

$$\Pi = \Pi_1 + \Pi_2 + \Pi_3. \tag{20}$$

Π_1 is the complementary energy of the shaft, Π_2 is the complementary energy of the tube, and Π_3 is the complementary energy of the adhesive. Π_1, Π_2, and Π_3 are given by

$$\Pi_1 = \pi \int_0^L \int_a^b \left[\frac{\sigma_{zz}^{(1)2}}{E_{l1}} + \frac{\sigma_{\theta\theta}^{(1)2}}{E_{t1}} - \frac{2\nu_{tl1}}{E_{t1}} \sigma_{zz}^{(1)} \sigma_{\theta\theta}^{(1)} + \frac{\tau_{rz}^{(1)2}}{G_1} \right] r \, dr \, dz \tag{21}$$

$$\Pi_2 = \pi \int_0^L \int_c^d \left[\frac{\sigma_{zz}^{(2)2}}{E_{l2}} + \frac{\sigma_{\theta\theta}^{(2)2}}{E_{t2}} - \frac{2\nu_{tl2}}{E_{t2}} \sigma_{zz}^{(2)} \sigma_{\theta\theta}^{(2)} + \frac{\tau_{rz}^{(2)2}}{G_2} \right] r \, dr \, dz \tag{22}$$

$$\Pi_3 = \pi \int_0^L \int_b^c \frac{1}{E(z)} \left[\sigma_{\theta\theta}^2 + 2(1+\nu)\tau_{rz}^2 \right] r \, dr \, dz. \tag{23}$$

For an isotropic system, Π_1 and Π_2 become

$$\Pi_1 = \pi \int_0^L \int_a^b \frac{1}{E_1} \left[\sigma_{zz}^{(1)2} + \sigma_{\theta\theta}^{(1)2} - 2\nu_1 \sigma_{zz}^{(1)} \sigma_{\theta\theta}^{(1)} + 2(1+\nu_1)\tau_{rz}^{(1)2} \right] r \, dr \, dz \tag{24}$$

$$\Pi_2 = \pi \int_0^L \int_c^d \frac{1}{E_2} \left[\sigma_{zz}^{(2)2} + \sigma_{\theta\theta}^{(2)2} - 2\nu_2 \sigma_{zz}^{(2)} \sigma_{\theta\theta}^{(2)} + 2(1+\nu_2)\tau_{rz}^{(2)2} \right] r \, dr \, dz. \tag{25}$$

Introducing expressions for stresses ($\sigma_{\theta\theta}^{(1)}$ and $\tau_{rz}^{(1)}$) in Π_1 and integrating the resulting expression over the radius, r, the complementary energy of the isotropic shaft becomes

$$\Pi_1 = \pi \int_0^L \left[A_1 \sigma_{zz}^{(1)2} + A_2 \left(\frac{d^2 \sigma_{zz}^{(1)}}{dz^2} \right)^2 + A_3 \frac{d^2 \sigma_{zz}^{(1)}}{dz^2} \sigma_{zz}^{(1)} + A_4 \left(\frac{d\sigma_{zz}^{(1)}}{dz} \right)^2 \right] dz, \tag{26}$$

where

$$A_1 = \frac{b^2}{2E_1}; \quad A_2 = \frac{b^6}{24E_1} \tag{27}$$

$$A_3 = \frac{-\nu_1 b^4}{4E_1}; \quad A_4 = \frac{(1+\nu_1)b^4}{8E_1}. \tag{28}$$

Downloaded At: 19:34 21 January 2011

Again, using the expressions for stresses ($\sigma_{zz}^{(2)}$, $\sigma_{\theta\theta}^{(2)}$, and $\tau_{rz}^{(2)}$) inΠ_2, and integrating the resulting expression over the radius, r, the energy functional for an isotropic tube becomes

$$\Pi_2 = \pi \int_0^L \Big[C_1 + C_2 \sigma_{zz}^{(1)2} + C_3 \sigma_{zz}^{(1)} + C_4 \left(\sigma_{zz}^{\prime\prime(1)} \right)^2 + C_5 \sigma_{zz}^{\prime\prime(1)} + C_6 \sigma_{zz}^{\prime\prime(1)} + C_7 \left(\sigma_{zz}^{\prime\prime(1)} \right) \Big] dz \tag{29}$$

Here, $\sigma_{zz}^{\prime\prime(1)} = \frac{d^2\sigma_{zz}^{(1)}}{dz^2}, \sigma_{zz}^{\prime(1)} = \frac{d\sigma_{zz}^{(1)}}{dz}$ and

$$C_1 = \frac{f^2(d^2 - c^2)}{2E_2} \tag{30}$$

$$C_2 = \frac{\rho^2(d^2 - c^2)}{2E_2}; \quad \rho = \frac{b^2}{(c^2 - d^2)} \tag{31}$$

$$C_3 = \frac{f\rho(d^2 - c^2)}{E_2} \tag{32}$$

$$C_4 = \frac{\rho^2 l_3}{4E_2}; \quad l_3 = \int_c^d \left(r^2 - d^2\right)^2 r\, dr \tag{33}$$

$$C_5 = \frac{-\nu_2 f\rho m_3}{E_2}; \quad m_3 = \int_c^d \left(r^2 - d^2\right) r\, dr \tag{34}$$

$$C_6 = \frac{-\nu_2 \rho^2 m_3}{E_2} \tag{35}$$

$$C_7 = \frac{(1 + \nu_2)\rho^2 n_3}{2E_2}; \quad n_3 = \int_c^d \frac{\left(r^2 - d^2\right)^2}{r}\, dr. \tag{36}$$

Similarly, using expressions for stresses (τ_{rz} and $\sigma_{\theta\theta}$) in Π_3 and integrating over the radius, r, the complementary energy in the FMGB adhesive becomes

$$\Pi_3 = \pi \int_0^L \left[\frac{B_1}{E(z)} \left(\frac{d^2\sigma_{zz}^{(1)}}{dz^2} \right)^2 + \frac{B_2}{E(z)} \left(\frac{d\sigma_{zz}^{(1)}}{dz} \right)^2 \right] dz, \tag{37}$$

where

$$B_1 = \frac{b^4(c^2 - b^2)}{8}; \quad B_2 = \frac{(1 + \nu_c) b^4 \ln(c/b)}{2}. \tag{38}$$

Downloaded At: 19:34 21 January 2011

The complementary energy in the whole assembly becomes

$$\Pi = \pi \int_0^L \left[\alpha_1 \sigma_{zz}^{(1)2} + \alpha_2(z) \left(\sigma_{zz}^{\prime\prime(1)} \right)^2 + \alpha_3 \sigma_{zz}^{\prime\prime(1)} \sigma_{zz}^{(1)} + \alpha_4(z) \left(\sigma_{zz}^{\prime(1)} \right)^2 \right] dz + \pi \int_0^L \left[\alpha_5 \sigma_{zz}^{\prime\prime(1)} + \alpha_6 \sigma_{zz}^{(1)} + \alpha_7 \right] dz \tag{39}$$

where the constant coefficients α_1, α_3, α_5, α_6, and α_7 and the variable coefficients $\alpha_2(z)$ and $\alpha_4(z)$ depend on geometrical and material properties and the loading conditions of the bonded joint, where

$$\alpha_1 = A_1 + C_2; \quad \alpha_2(z) = A_2 + \frac{B_1}{E(z)} + C_4; \quad \alpha_3 = A_3 + C_6; \tag{40}$$

$$\alpha_4(z) = A_4 + \frac{B_2}{E(z)} + C_7; \quad \alpha_5 = C_5; \quad \alpha_6 = C_3; \quad \alpha_7 = C_1. \tag{41}$$

The above integral Π can be re-written as a function of longitudinal stress $\sigma_{zz}^{(1)}$ and its derivatives as

$$\Pi = \int_0^L \Psi \left(\sigma_{zz}^{(1)}, \sigma_{zz}^{\prime(1)}, \sigma_{zz}^{\prime\prime(1)}, z \right) dz. \tag{42}$$

We now need the differential equation satisfied by the function $\sigma_{zz}^{(1)}$ which minimises the above functional. Performing variational calculus on the above functional yields

$$\frac{\partial \Psi}{\partial \sigma_{zz}^{(1)}} - \frac{d}{dz} \left(\frac{\partial \Psi}{\partial \sigma_{zz}^{\prime(1)}} \right) + \frac{d^2}{dz^2} \left(\frac{\partial \Psi}{\partial \sigma_{zz}^{\prime\prime(1)}} \right) = 0. \tag{43}$$

Manipulating the above equation results in the following differential equation which can be solved with the stress boundary conditions and stress-free end conditions given by Eqs. (13) and (14) respectively. Note that the stress continuity at the interfaces are automatically satisfied.

$$\alpha_2(z) \frac{d^4 \sigma_{zz}^{(1)}}{dz^4} + 2\alpha_2'(z) \frac{d^3 \sigma_{zz}^{(1)}}{dz^3} + (\alpha_3 - \alpha_4(z) + \alpha''_2(z)) \frac{d^2 \sigma_{zz}^{(1)}}{dz^2} + \alpha_4'(z) \frac{d\sigma_{zz}^{(1)}}{dz} + \alpha_1 \sigma_{zz}^{(1)} + \frac{\alpha_6}{2} = 0 \tag{44}$$

5. RESULTS AND DISCUSSION

Stress analyses of the isotropic bonded system have been carried out in two stages under the same axial tensile load, P, with bondlength $L = 50\,\text{mm}$. Initially, the joint analysed consisted of the aluminium

Downloaded At: 19:34 21 January 2011

TABLE 1 Geometric and Material Properties of Adhesive and Adherends

Item	Material	E [GPa]	ν	b [mm]	c [mm]	d [mm]	f [MPa]
Shaft	AU 4G	75	0.3	11	–	–	1000
Tube	AU 4G	75	0.3	–	11.2	12.2	–
Adhesive	Araldite AV119	2.7	0.35	11	11.2	–	–

alloy shaft and tube with a FMGB adhesive. The geometrical and material properties of the aluminium alloy adherends used in the analyses are given in Table 1. The FMGB adhesive having the modulus function E_{f1} with $E_o = 280\,\text{MPa}$ and $E_m = 2700\,\text{MPa}$ was used in the analysis. In the second stage, the joint analysed consisted of the same aluminium alloy adherends and AV119 adhesive whose properties are given in Table 1. (Aluminium adherends and AV119 adhesive properties were taken from Nemes *et al.* [23].) The shear and peel stresses both at the midplane and at the interfaces of the FMGB adhesive joint were studied and compared with the MMB adhesive joint. The distributions of shear and peel stresses at the midplane of the adhesive are shown in Figs. 5 and 6, respectively. As imposed, the shear stress vanishes at the overlap ends and its peak appears close to the tube overlap end. The shear stress distribution is not symmetrical about

Downloaded At: 19:34 21 January 2011

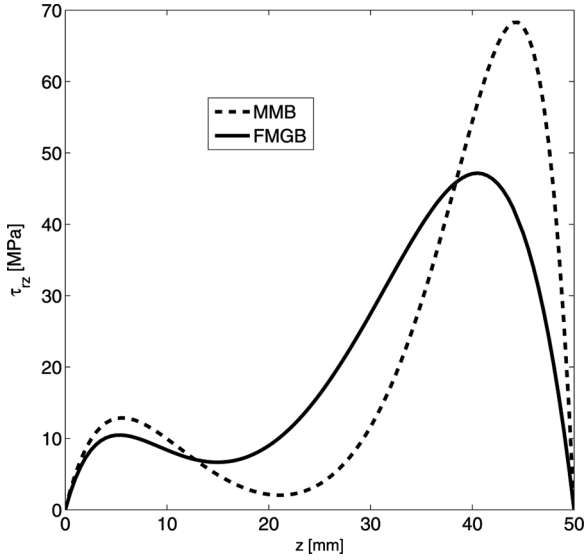

FIGURE 5 Shear stress distribution at the midplane of the adhesive layer.

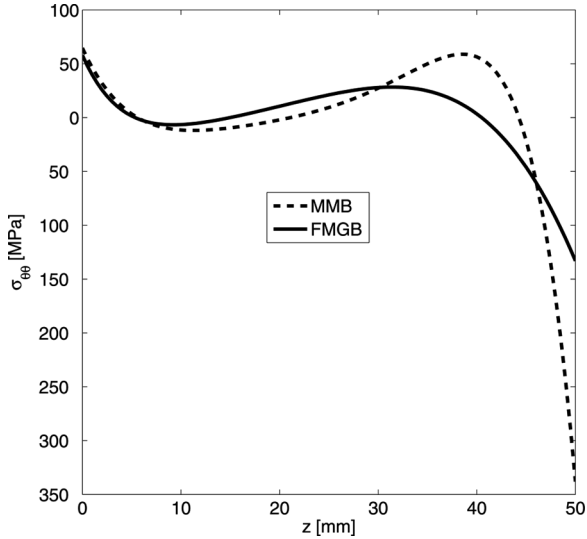

FIGURE 6 Peel stress distribution at the midplane of the adhesive layer.

Downloaded At: 19:34 21 January 2011

the mid-bondline because of the stiffness mismatch between shaft and tube. On the other hand, peel stress peaks appear at the ends of the overlap. Because of the stress equilibrium conditions, it can be expected that the shear stress gradient is associated with the peel stress gradient across the thickness of the adhesive layer. The peel stress distribution is not anti-symmetric about the mid-bondline for the same reason stated above. The peak peel stress appears at the tube overlap end. It is obvious from these figures that the shear and peel stress intensities are minimum and their distributions along the bondline are more uniform in the FMGB adhesive than those of a MMB adhesive joint. For the parameters used here, the shear stress peak reduces by 30% and the peel stress peak reduces by 58% by employing a FMGB adhesive in lieu of a MMB adhesive. If the modulus function, E_{f4}, is employed (*i.e.*, MMB), stress distributions in the adhesive agree with the stress distribution predicted by Shi and Cheng [16].

5.1. Effect of Bondlength (*L*)

To investigate the effects of bondlength on adhesive stresses, analyses have been carried out by varying the bondlength from 10 to 100 mm with a FMGB adhesive of modulus function E_{f1} and also with a

MMB adhesive under the same axial load, P. Figures 7 and 8 show the shear and peel stress distributions at the midplane of the adhesive layer respectively. For a small bondlength, say $L \leq 20$ mm, the peak shear stress occurs almost at the mid-bondlength in both FMGB and MMB adhesives and its distribution is parabolic. For bondlength $L \leq 10$ mm, shear and peel stress distributions are more severe in

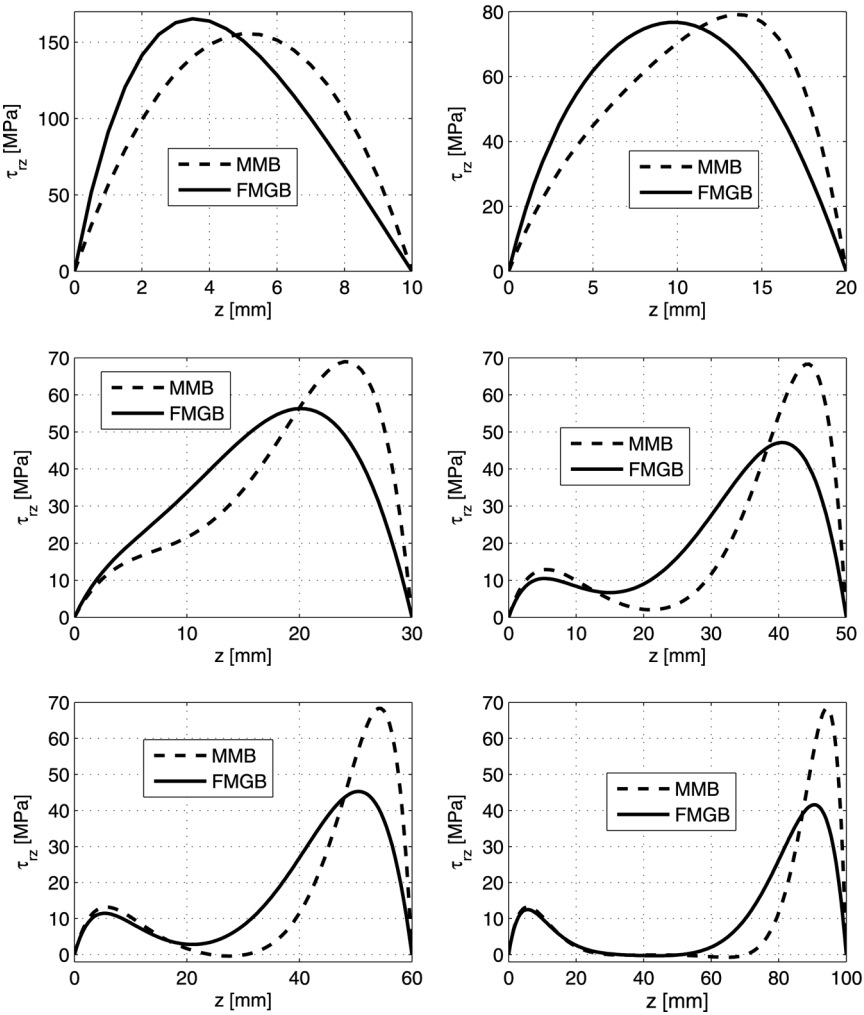

FIGURE 7 Shear stress distribution at the midplane of the adhesive layer as a function of the bondlength.

Downloaded At: 19:34 21 January 2011

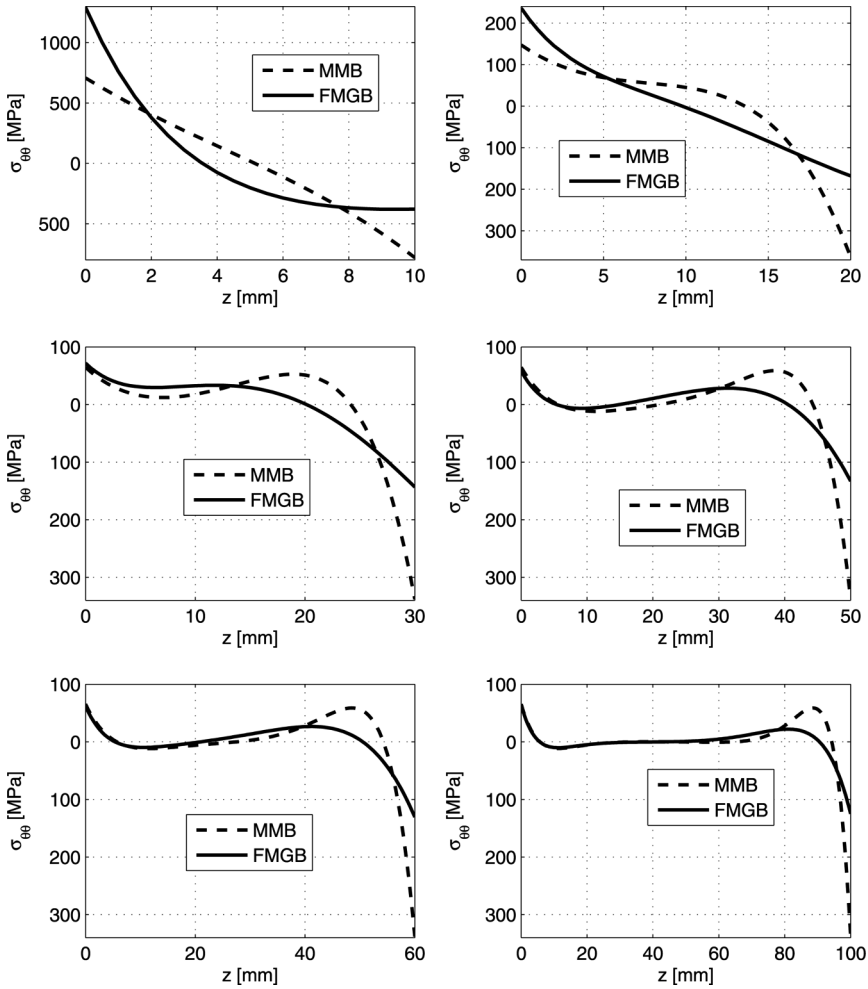

FIGURE 8 Peel stress distribution at the midplane of the adhesive layer as a function of the bondlength.

the FMGB adhesive than in the MMB adhesive. As the bondlength increases, shear and peel peak stresses reduce and their distributions become more uniform. With increase of bondlength, the shear stress peak shifts towards the tube overlap end. The shear and peel peak stresses reduce continuously with increase of bondlength (up to $L = 100$ mm), whereas they do not reduce appreciably beyond a particular length ($L = 50$ mm in this case) in the MMB adhesive.

Downloaded At: 19:34 21 January 2011

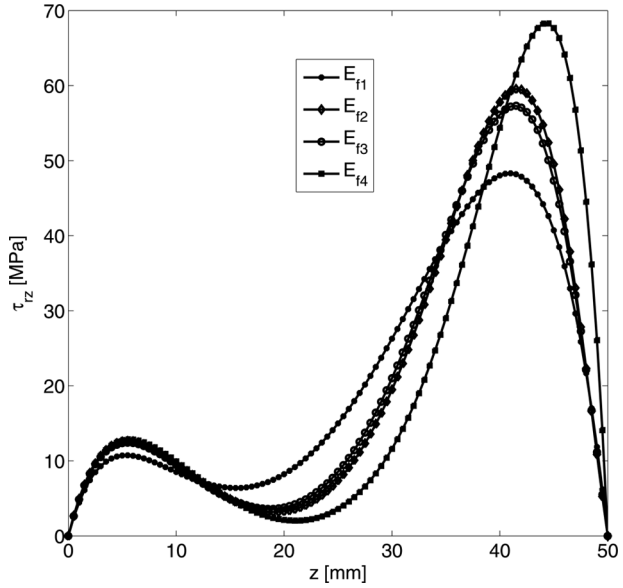

FIGURE 9 Shear stress distribution at the midplane of the adhesive for different modulus function profiles.

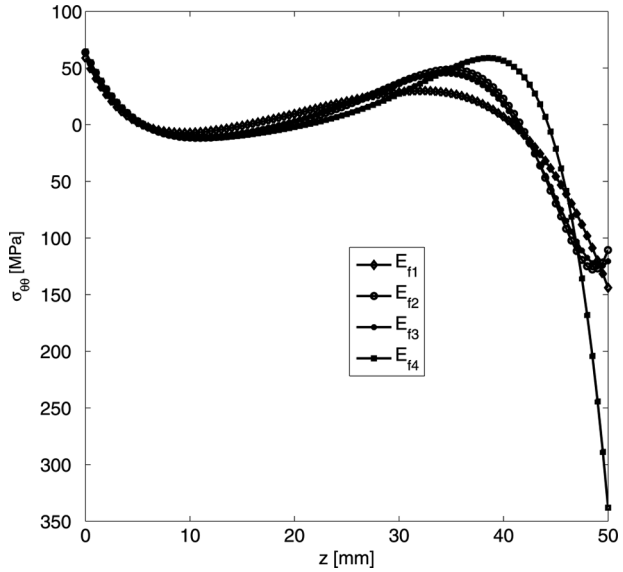

FIGURE 10 Peel stress distribution at the midplane of the adhesive for different modulus function profiles.

Downloaded At: 19:34 21 January 2011

5.2. Effect of Modulus Function

Different modulus function profiles have been examined under the same axial tensile load, P, to reduce the shear and peel peak stresses and their gradients in the FMGB adhesive. The shear and peel stress distributions for different modulus functions are shown in Figs. 9 and 10, respectively. The shear stress intensity is less and its distribution is more uniform for the modulus function E_{f1} while the peel stress intensity is less for the modulus function E_{f3}. If we choose a stiff MMB adhesive to ensure higher shear strength, it would fail due to high peel stress. Unlike the MMB adhesive, the modulus function of

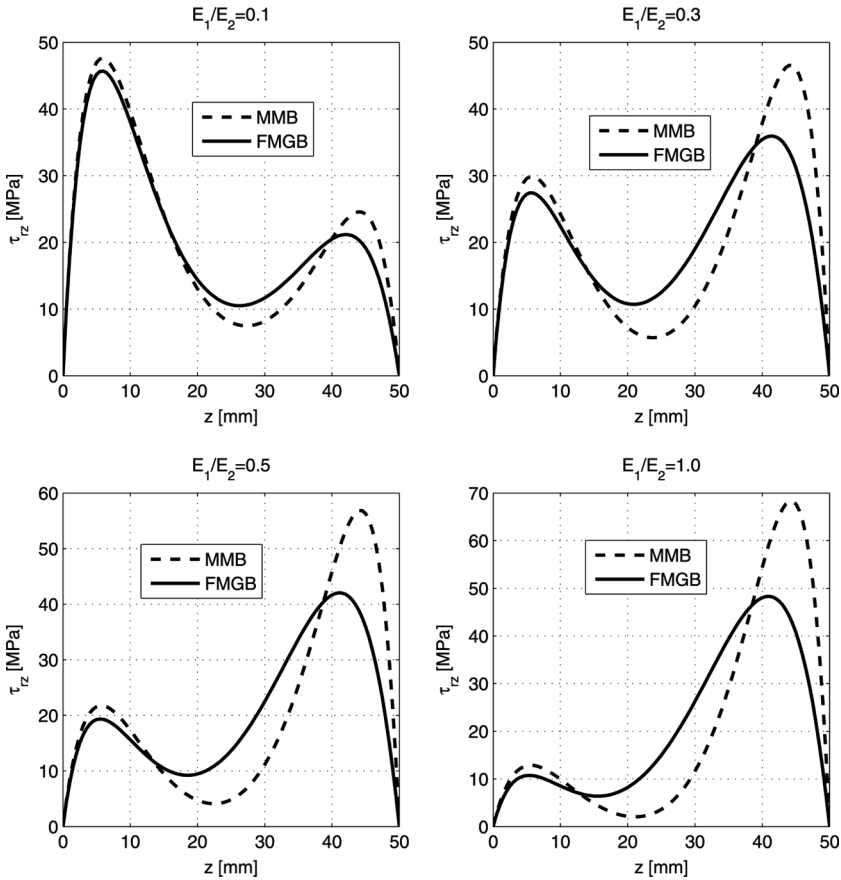

FIGURE 11 Shear stress distribution at the midplane of the adhesive as a function of the stiffness mismatch.

Downloaded At: 19:34 21 January 2011

the FMGB adhesive can be so tailored, simultaneously, as to achieve both shear and peel strengths.

5.3. Effect of Stiffness Mismatch

Analyses have been carried out with modulus function E_{f1} for different E_1/E_2 ratios under the axial load P. Figures 11 and 12 show the shear stress distribution at the midplane of the adhesive as a function of stiffness mismatch between shaft and tube. When E_1 is very small compared with E_2, say $E_1 = 0.1E_2$, the shear stress peak appears close to the shaft overlap end of the adhesive. As we increase E_1, when

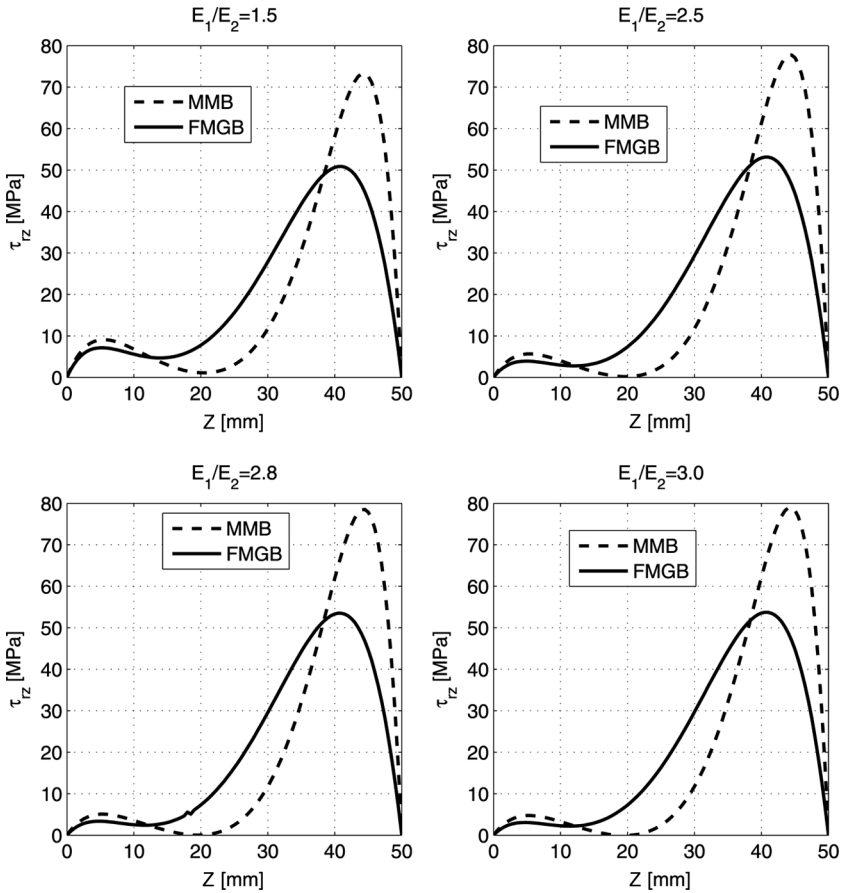

FIGURE 12 Shear stress distribution at the midplane of the adhesive as a function of the stiffness mismatch.

Downloaded At: 19:34 21 January 2011

$E_1 \simeq 0.2E_2$, the shear stress distribution is symmetric about the mid-bondline. This is the optimum ratio at which the shear stress peak is mimimum in the bondline. If we increase the modulus ratio beyond $E_1/E_2 = 0.2$, the shear stress distribution loses its symmetricity about its mid-bondline and the shear stress peak increases close to the tube overlap end of the bondline. However, the shear stress peak close to the shaft end of the bondline decreases and the distribution becomes more uniform. Figures 13 and 14 show the peel stress distribution at the midplane of the adhesive as a function of stiffness mismatch. At a small E_1/E_2 ratio, say 0.1, the peel stress peak appears at the shaft overlap end of the bondline. As we increase this ratio, the distribution becomes anti-symmetric at about 0.2. This is the optimum ratio at

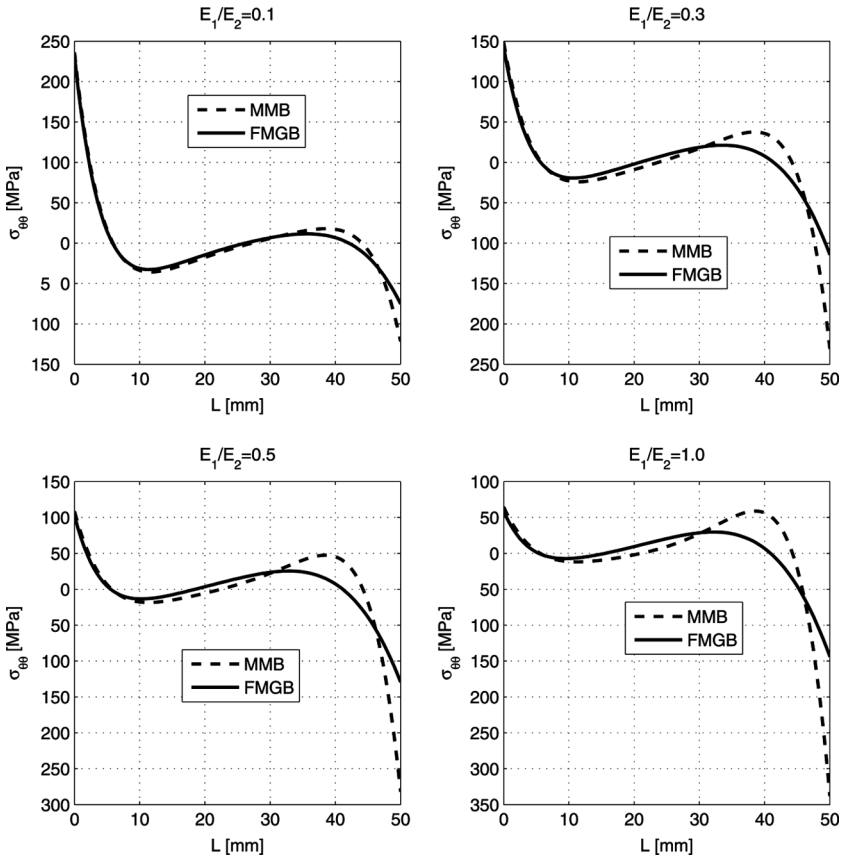

FIGURE 13 Peel stress distribution at the midplane of the adhesive as a function of the stiffness mismatch.

Downloaded At: 19:34 21 January 2011

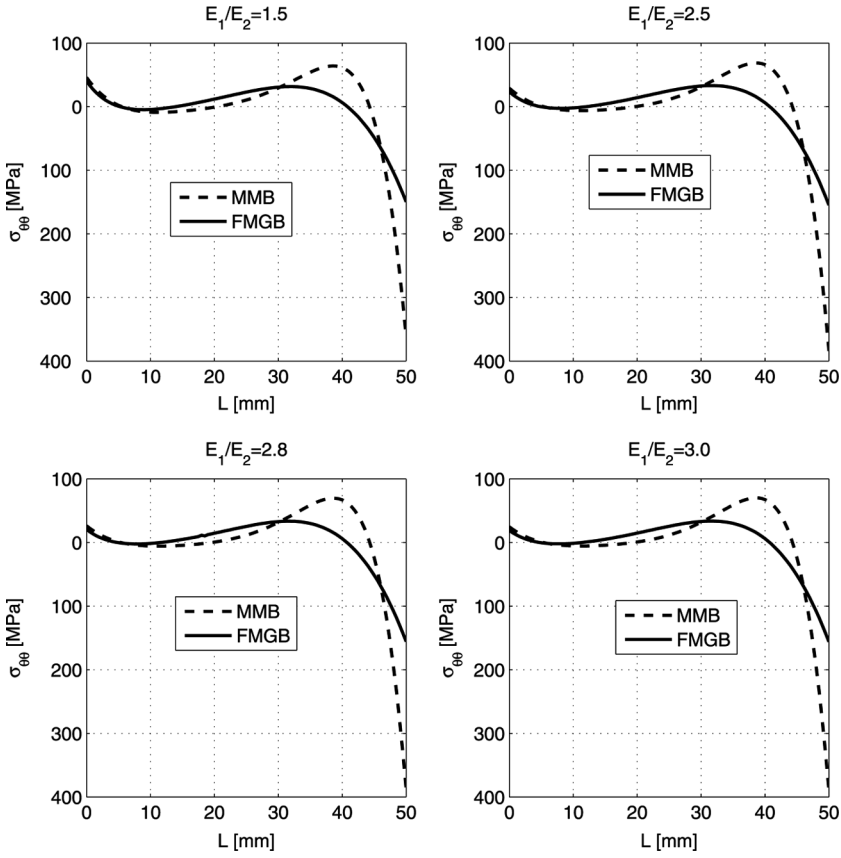

FIGURE 14 Peel stress distribution in the adhesive as a function of the stiffness mismatch.

Downloaded At: 19:34 21 January 2011

which we have minimum peel stress intensity in the adhesive. As we increase this ratio further, peel stress distribution loses its anti-symmetricity and its peak appears at the tube overlap end of the adhesive. The peel stress peak increases with increase of the E_1/E_2 ratio at the tube overlap end, while the intensity decreases at the shaft end of the bondline. We can't always choose this modulus ratio since it is based on the functional requirements of the materials to be joined.

5.4. Effect of Adhesive Thickness

Analyses were performed with the modulus function profile E_{f1}, varying the thickness of the adhesive while keeping the shaft diameter and

the thickness of the tube constant. The influence of adhesive thickness variation on the shear and peel stresses and their distributions are shown in Figs. 15 and 16, respectively. As the thickness of the adhesive increases, both shear and peel peak stresses reduce and their distributions become more uniform in both FMGB and MMB adhesive joints. With increase of adhesive thickness, the shear stress peak shifts towards mid-bondline.

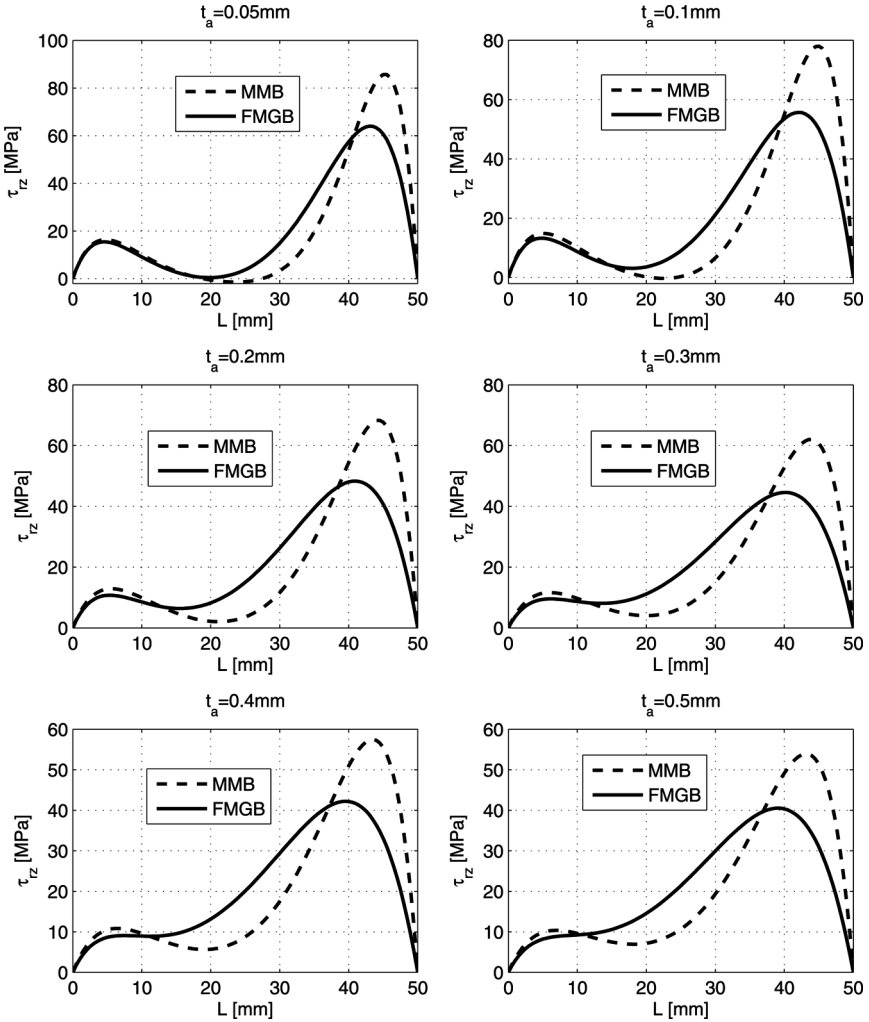

FIGURE 15 Shear stress distribution at the midplane of adhesive as a function of the bondline thickness.

Downloaded At: 19:34 21 January 2011

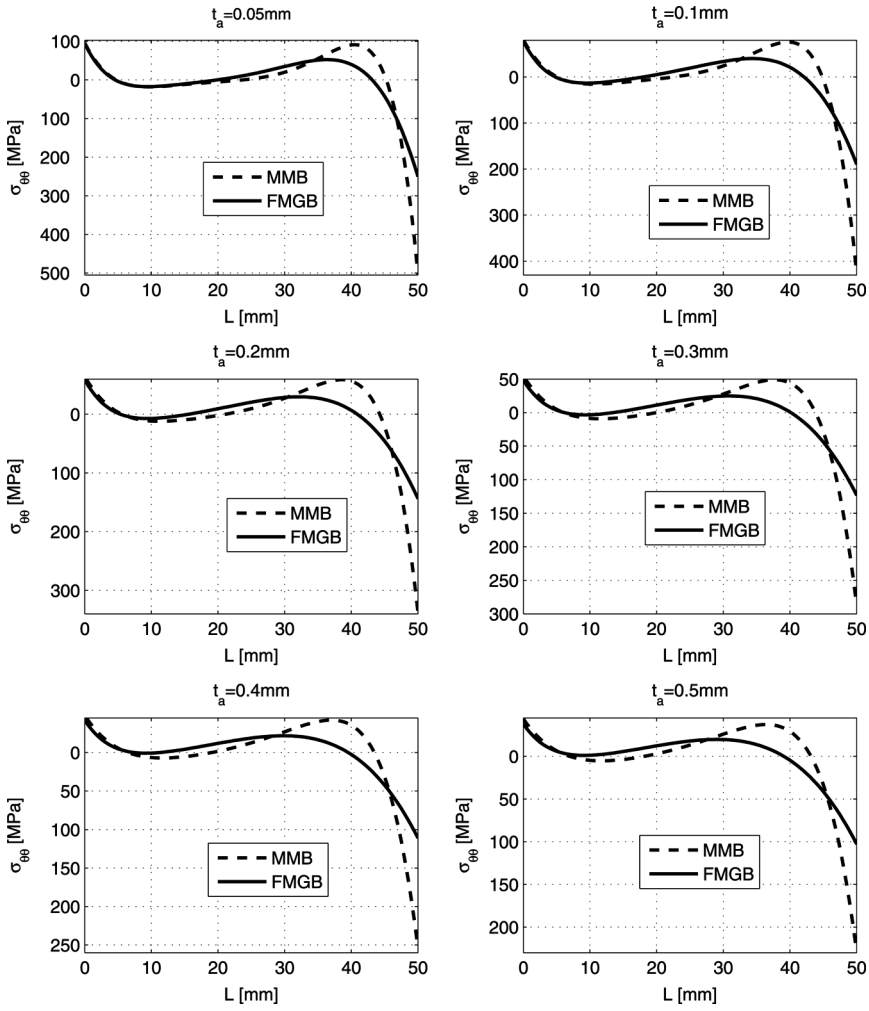

FIGURE 16 Peel stress distribution at the midplane of the adhesive as a function of the bondline thickness.

6. CONCLUSIONS

A novel concept of functional grading of adhesive modulus has been implemented, in order to reduce the peak stresses and their non-uniform distribution in the adhesive of a shaft-tube bonded joint based on a variational method. Three functionally modulus grading profiles were examined and the results were compared with

Downloaded At: 19:34 21 January 2011

conventional MMB adhesive joints. Stress analysis indicates more reduction in shear and peel peak stresses and their gradients in the overlap ends of the bondline for the exponential modulus function profile. For this modulus profile, the shear stress peak is reduced by 30% and the peel stress peak is reduced by 58%. The reduction in shear and peel stress concentrations would significantly improve joint strength and performance. Parametric studies have been conducted by selectively perturbing the geometrical and material properties of the bonded system in order to reduce the shear and peel peak stresses and their gradients.

REFERENCES

[1] Lubkin, J. L. and Reissner, E., *Journal of Applied Mechanics* **78**, 1213–1221 (1958).
[2] Volkersen, O., *Luftfahrtforschung* **15**, 41–47 (1938).
[3] Goland, M. and Reissner, E., *J. of Applied Mechanics, Trans ASME* **66**, A17–27 (1944).
[4] Hart-Smith, L. J., *J. Aerospace Eng. G. IMechE.* **209**, 105–129 (1995).
[5] Wooley, G. R. and Carver, D. R., *J. Aircraft* **8**, 817–820 (1971).
[6] Adams, R. D. and Peppiatt, N. A., *J. Strain Anal.* **9**, 185–196 (1974).
[7] Crocombe, A. D. and Adams, R. D., *J. Adhesion* **13**, 141–155 (1981).
[8] Adams, R. D. and Peppiatt, N. A., *J. Adhesion* **9** (1), 1–18 (1977).
[9] Nagaraja, Y. R. and Alwar, R. S., *Computers Structures* **11**, 621–627 (1980).
[10] Harris, J. A. and Adams, R. D., *Int. J. Adhesion Adhesives* **4**, 65–78 (1984).
[11] Pickett, A. K. and Hollaway, L., *Composite Structures* **4**, 135–160 (1985).
[12] Oplinger, D. W., Army materials technology laboratory report MTL TR 91–23 (1991).
[13] Tsai, M. Y. and Morton, J., Center for adhesive and sealant science, VPI, Report CASS/ESM-92-8 (1993).
[14] Deb, A., Malvade, I., Biswas, P., and Schroeder, J., *Int. Journal of Adhesion and Adhesives* **28**, 1–15 (2007).
[15] Allman, D. J., *Quart. J. Mech. Appl. Math.* **30**, 415–436 (1977).
[16] Shi, Y. P. and Cheng, S., *J. Eng. Mech.* **119** (3), 584–602 (1993).
[17] Lindon, J., Perez, B., Martinez, M. A., and Madrid, M., *J. Adhesion Sci. Techonol.* **19** (1), 41–56 (2005).
[18] Pugno, N. and Carpinteri, A., *Transactions of the ASME* **70**, 832–839 (2003).
[19] Imanaka, M., Kishimoto, W., Okita, K., Nakayama, H., and Nagai, H., *Int. J. Fracture* **41**, 223–234 (1989).
[20] Nayeb-Hashemi, H., Rosettos, J. N., and Melo, A. P., *Int. J. Adhesion and Adhesives* **17**, 55–63 (1997).
[21] Thomsen, O. T., *Composite Structures* **21**, 249–259 (1992).
[22] Kim, Y. G., Oh, J. H., and Lee, D. G., *J. Composite Materials* **33** (20), 1897–1917 (1999).
[23] Nemes, O., Lachaud, F., and Mojtabi., *Int. J. Adhesion and Adhesives* **26**, 474–480 (2006).
[24] Her, S. C., *Compos. Struct.* **47**, 673–678 (1999).
[25] Apalak, M. K., *J. Adhes. Sci. Technol.* **13** (11), A17–A27 (1999).
[26] Penado, F. E., *Int. J. Fract.* **105** (1), 1–25 (2000).
[27] Erdogan, F. and Ratwani, M., *J. Compos. Mater.* **5**, 378–393 (1971).

Downloaded At: 19:34 21 January 2011

[28] Amijima, S. and Fujii, T., *Int. Journal of Adhesion and Adhesives* **9** (3), 155–160 (2006).
[29] Kim, J. S., Kim, C. G., and Hong, C. S., *Comps. Struct.* **51** (3), 285–299 (2001).
[30] Lang, T. P. and Mallick, P. K., *Int. Journal of Adhesion and Adhesives* **19**, 257–271 (1999).
[31] Lang, T. P. and Mallick, P. K., *Int. Journal of Adhesion and Adhesives* **18** (3), 167–177 (1998).
[32] Tsai, M. Y. and Morton, J., *Compos. Struct.* **32** (1–4), 123–131 (1995).
[33] Krieger, R. B., In: *Adhesively Bonded Joints: Testing, Analysis, and Design, ASTM STP* **981**, 264–275 (1988).
[34] Sadek, M. M., *Industrial Applications of Adhesive Bonding*, (Elsevier Applied Science Publishers, London, UK, 1987).
[35] Ganesh, V. K. and Choo, T. S., *J. Composite Materials* **36** (14), 1757–1767 (2002).
[36] Boss, J. N., Ganesh, V. K., and Lim, C. T., *Composite Struct.* **62**, 113–121 (2003).
[37] Pires, I., Quintino, L., Durodola, J. F., and Beevers, A., *Int J. Adhesion and Adhesives* **23**, 215–223 (2003).
[38] Pires, I., Quintino, L., and Mirinda, R. M., *J. Adhesion Sci. Techonol.* **20** (1), 19–36 (2006).
[39] Fitton, M. D. and Broughton, J. G., *Int. Journal of Adhesion and Adhesives* **25**, 329–336 (2005).
[40] Temiz, S., *J. Adhesion Sci. Techonol.* **20** (14), 1547–1560 (2006).
[41] Kumar, S. and Pandey, P. C., *J. Adhesion Sci. Techonol.* **0**, 1–31 (2009).
[42] Kumar, S., *Int. Journal of Adhesion and Adhesives* **29** (8), 785–795 (2009).
[43] Da Silva, L. F. M. and Adams, R. D., *Int. Journal of Adhesion and Adhesives* **27**, 216–227 (2007).
[44] Mengel, R., Haberle, J., and Schlimmer, M., *Int. Journal of Adhesion and Adhesives* **27**, 568–573 (2007).
[45] Chalkley, P. and Rose, F., *Int. Journal of Adhesion and Adhesives* **21**, 241–247 (2001).

Downloaded At: 19:34 21 January 2011